



POROUS STRUCTURE OF PAN-BASED ACTIVATED CARBON FIBERS

ZHENYU RYU,* JINGTANG ZHENG and MAOZHANG WANG

Institute of Coal Chemistry, Academia Sinica, P.O. Box 165, Taiyuan 030001, People's Republic of China

(Received 2 September 1997; accepted in revised form 14 November 1997)

Abstract—The porous structure of polyacrylonitrile (PAN)-based activated carbon fibers (ACFs) was studied by means of nitrogen adsorption over a wide range of relative pressure and scanning electron microscopy (SEM). The specific surface area of samples was evaluated using the standard BET method. The micropore volume was obtained from the Dubinin–Astokhov and Horvath–Kawazoe equations. An average micropore size was calculated from the Dubinin–Radushkevich equation. The pore size distributions of the samples were calculated by employing the regularization method according to Density Functional Theory (DFT). It was shown that adsorption measurement provides profound insight into the structural heterogeneity of porous carbonaceous adsorbents. The analysis results by means of different methods had a good consistence with one another. © 1998 Elsevier Science Ltd. All rights reserved.

Key Words—A. Activated carbon, B. carbonization, C. adsorption, scanning electron microscopy (SEM), D. porosity.

1. INTRODUCTION

Activated carbon fiber (ACF) is a novel and fibrous adsorbent which has been developed by carbonization and activation of organic fibers. Its unique properties are attracting attention in fundamental research and in the development of applications [1]. The advantages of ACF are the smaller fiber diameter (which minimizes diffusion limitations and allows rapid adsorption/desorption), more concentrated pore size distribution and excellent adsorption capacity at low concentration of adsorbates compared with conventional activated granular/powder carbons. The porosity of ACF is developed during activation, normally by partial gasification in steam and/or carbon dioxide and it is influenced by many factors, such as the degree of activation and the conditions used for carbonization. Although the porous structure of the resulting ACF mainly depends on the activation agents and activation conditions, the nature of the raw material greatly influences the properties of the product. Typically, ACF is a kind of micropore carbonous adsorbent exhibiting slit-shaped pores. This feature is a source of their high adsorption capacities, which makes them suitable as adsorbents, catalysts and catalyst supports. Adsorption properties are associated with their porous structure and surface structural characteristics. Nitrogen is contained in the structure of polyacrylonitrile (PAN)-based ACFs, this introduces an interesting function as adsorbent and catalyst [2].

In the present work, PAN-based ACFs are prepared and the results of porous structure parameters are investigated. Nitrogen adsorption measurements

were used to evaluate the specific surface area, micropore surface area, micropore volume and pore size distribution for PAN-based ACFs. The specific surface area of samples studied was calculated from the BET method [3]. The micropore surface area and volume were obtained from the Dubinin–Astakhov and Horvath–Kawazoe equations [4,5]. The pore size distribution of the samples was calculated by employing the regularization method according to Density Functional Theory (DFT) [6–8]. Using scanning electron microscopy (SEM), the porosity of ACFs at both the fiber surface and fiber cross-section was imaged. Analysis of these quantities allowed for the study of the development of porous structure in PAN-based ACFs.

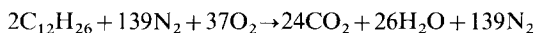
2. EXPERIMENTAL

2.1 Sample preparation

PAN-based ACF samples were prepared in our laboratory by continuous vertical synchronism carbonization and activation apparatus in steam, carbon dioxide and nitrogen gas atmosphere, the details of which are described elsewhere [9]. Carbon fibers (CF) obtained after carbonization at round 1000°C have only a very limited pore volume and their surface must be activated by a suitable treatment. ACFs were not carbonized independently, activation and carbonization occurred at the same time. CF and ACF had to be prepared in an inert gas atmosphere, bottled nitrogen gas was used in the conventional process. In our process we developed a new method to produce inert gas which contained an oxidative gas (steam, carbon dioxide and low concentration oxygen) as activating agent, and formed a

*Corresponding author.

unique characteristic of our process. Kerosene was used in the procedure, the reaction formula is as followings:



The starting material (preoxidative PAN fiber) was submitted to the carbonization and activation reaction in the vertical apparatus in a temperature interval of 500–1000°C in steam, carbon dioxide, low concentration oxygen and inert nitrogen gas atmosphere. During the activation procedure, the apparatus was maintained at a low concentration of oxygen (<2 ppm), thus the activation reaction proceeded rapidly. At the same time the apparatus was of the vertical type, the gas produced by the carbonization and activation reaction was rapidly discharged to outside by the draft effect, thus the activation solid-gas reaction extended forward. PAN-based ACF samples with different specific surface areas were prepared by controlling the contact degree between the solid and activating agent or the feeding speed.

2.2 Adsorption measurements and SEM techniques

A Micromeritics ASAP 2000 accelerated surface area and porosimetry apparatus (Micromeritics Ins. Corp.) was used to measure nitrogen adsorption isotherms at 77.4 K in the range of relative pressure from 10^{-6} to 1. High purity (99.99%) nitrogen was used; before the measurement all samples were out-gassed at 300°C for 2 hours.

Porous structural observations of PAN-based ACF samples at both the fiber surface and fiber cross-section were obtained by using a Amray 1910 field emission scanning electron microscope.

3. RESULTS AND DISCUSSION

3.1 Adsorption isotherms

Nitrogen adsorption is a standard procedure for the determination of porosity of carbonaceous adsorbents. The adsorption isotherm is the information source about the porous structure of the adsorbent, heat of adsorption, characteristics of physics and

chemistry and so on. The definition of pore size follows the recommendations of IUPAC: micropore width less than 2 nm; mesopore width from 2 to 50 nm; and macropore width greater than 50 nm. Micropores can be divided into ultramicropores (width less than 0.7 nm) and supermicropores (width from 0.7 to 2 nm) [10]. Nitrogen adsorption isotherms for PAN-based ACF samples are of type I in the BDDT classification [10] except for samples A4 and A5, as illustrated in Fig. 1. Type I isotherms are characterized by a plateau which is nearly horizontal, and which may cut the $P/P_0=1$ axis sharply or may show a “tail” as saturation pressure is approached. The initial part of the type I isotherm for carbonaceous adsorbents represents micropore filling, and the slope of the plateau at high relative pressure is due to multilayer adsorption on the nonmicroporous surface, i.e. in mesopores, in macropores and on the external surface [10]. From this point of view, it is indicated that ACFs are essential microporous adsorbents. The exception of sample A4 suggests that there are some meso- and macropores in its structure. The volume filling of macropores by the mechanism of capillary condensation of vapor takes place at relative pressure close to unity. The nitrogen adsorption isotherm for sample A5 is of type IV which indicates that sample A5 is mesoporous. Thus PAN-based ACF samples with different porous structure can be prepared by controlling the degree of activation. The porous structure parameters derived from nitrogen adsorption isotherms analysis are listed in Table 1. The micropore volume and average pore width of PAN-based ACF both increase with the degree of activation, as expected.

3.2 Horvath–Kawazoe equation, DFT and SEM results

An alternative method proposed by Horvath and Kawazoe [5] was to calculate an average potential function inside the micropore, relating fluid–fluid and solid–fluid interaction of an adsorbed molecule to its free energy change upon adsorption. The resulting relation between filling pressure and slit-shaped pore

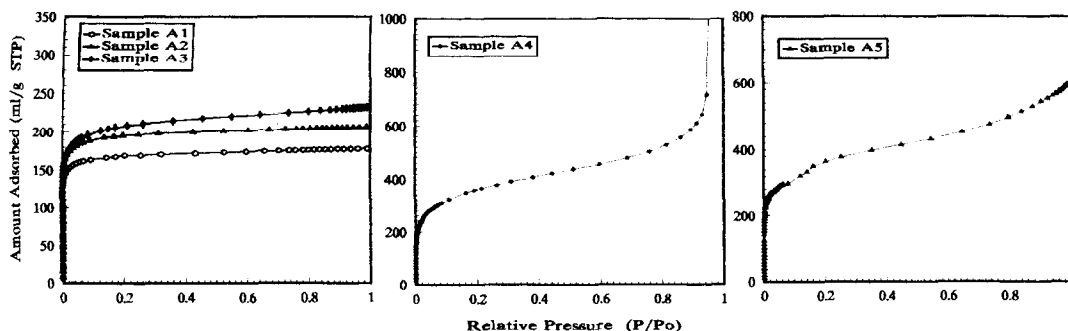


Fig. 1. Nitrogen adsorption isotherms for PAN-based ACFs at 77.4 K

Table 1. Porous structure parameters of PAN-based ACFs

Sample	S_{BET} ($\text{m}^2 \text{g}^{-1}$)	$V_{0.95}$ (ml g^{-1})	D_{aver} (nm)	Dubinin–Astakhov			Horvath–Kawazoe	
				S_{mi} ($\text{m}^2 \text{g}^{-1}$)	V_{mi} (ml g^{-1})	n	V_{mi} (ml g^{-1})	MPD (nm)
A1	576	0.27	1.90	561	0.22	9.9998	0.250	0.51
A2	673	0.32	1.89	629	0.25	9.9998	0.297	0.53
A3	738	0.36	1.94	651	0.26	6.1154	0.294	0.61
A4	1241	1.10	3.57	998	0.45	2.7819	0.480	0.73
A5	1265	0.89	2.69	1008	0.425	3.1231	0.425	0.63

S_{BET} : specific surface area by BET method; $V_{0.95}$: the total pore volume estimated at relative pressure 0.95; D_{aver} : according to the cylindrical pore model, $D_{\text{aver}} = 4V_{0.95}/S_{\text{BET}}$; S_{mi} : micropore surface area; V_{mi} : volume of micropore; n : exponent of Dubinin–Astakhov (0–9.9999); MPD : median pore diameter.

width is:

$$RT \ln(P/P_0) = K \frac{N_a A_a + N_A A_A}{\sigma^4 (L-d)} \times \left[\frac{\sigma^4}{3(L-d/2)^3} - \frac{\sigma^{10}}{9(L-d/2)^9} - \frac{\sigma^4}{3(L-d/2)^3} + \frac{\sigma^{10}}{9(d/2)^9} \right]$$

where K is Avogadro's number, σ is the zero interaction energy fluid–solid nuclear separation distance, L is pore width, d is the mean fluid–solid molecule diameter, N_a and N_A are the monolayer number of adsorbent and adsorbate, and A_a and A_A are Kirkwood–Muller dispersion constants for adsorbate–adsorbate and adsorbent–adsorbate interaction. The Horvath–Kawazoe method is an improvement over the Kelvin approach in that it acknowledges the strong adsorbent–adsorbate attractive forces in micropores [11]. The method is effective for calculation of molecular sieve pore or ultramicropore size distribution. The ultramicropore size distributions for PAN-based ACF samples according to the Horvath–Kawazoe method are shown in Fig. 2. From the differential pore volume plots, the ultramicropores less than 0.7 nm are present which lead to selectivity of adsorption (molecular sieve effect). The average micropore diameter is observed to increase with increasing surface area, pore size distribution becomes broader with increasing surface area suggesting that pore widening and pore generation occur cooperatively or that pores are generated over a broad activation range and pore widening for some pores occurs at the expense of smaller pores [12].

A sample of porous solid may be characterized by

its pore size distributions. Each pore size present will contribute to the total adsorption isotherm in proportion to the fraction of total area or pore volume of the sample that it presents. The experimental adsorption isotherm measured on a sample of porous solid is the aggregate of the isotherm for the individual pores that make up the pore structure of the solid (if it is assumed that the external surface area is much smaller than the surface area of the pores). In mathematical terms, the experimental isotherm is the integral of the single pore isotherm multiplied by the pore size distribution. For a slit-shaped pore, this can be written as [6–8]:

$$N(p) = \int_{H_{\min}}^{H_{\max}} f(H) \rho(p, H) dH$$

where $N(p)$ is the number of moles adsorbed at a pressure p , H_{\min} and H_{\max} are the widths of the smallest and largest pores present (where the pore width is the distance between the nuclei of carbon atoms on opposing pore walls), and $\rho(p, H)$ is the molar density of nitrogen at pressure p in a pore of width H . The pore size distribution, $f(H)$, is the distribution of pore volumes as a function of pore width. In this approach, the individual model pore isotherm $\rho(p, H)$ comes from the molecular model for nitrogen adsorption on the basis of nonlocal or smoothed density approximation.

The pore size distributions obtained by means of the regularization method proposed by Micromeritics Ins. Corp. support these findings, as can be seen in Fig. 3. Sample A2 possesses a reasonable amount of micropores which are bimodal, with a small fraction

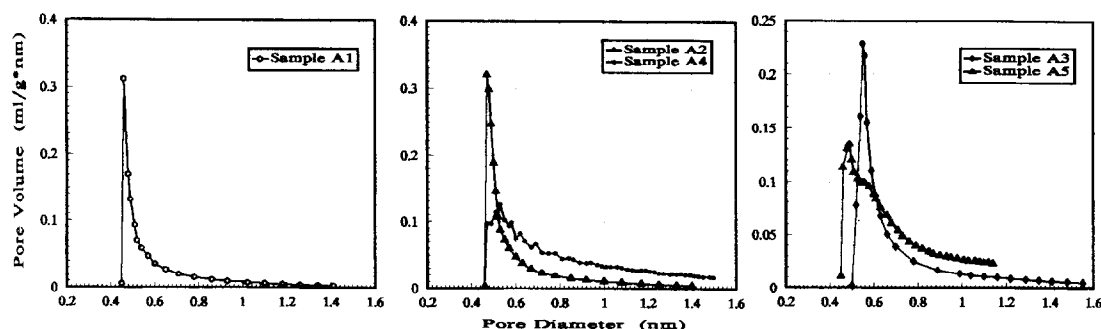


Fig. 2. Ultramicropore size distributions of PAN-based ACFs by Horvath-Kawazoe equation

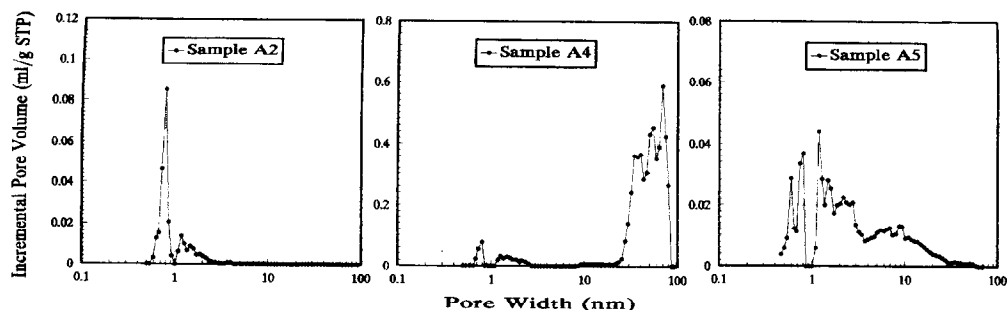


Fig. 3. Pore size distributions of PAN-based ACFs

of mesopores almost but not quite macropores. The sample A4 is mesoporous, with the same bimodal micropores as the sample A2 and with a small fraction of macropores. The sample A5 is also mesoporous, with the trimodal micropores almost not macropores.

A commercial Amray 1910 field emission scanning electron microscopy (SEM) is employed for the study of the samples under ambient conditions. The surface relief is expressed with increasing shades of gray where lighter regions are "hills" and darker regions are "valleys". The electron micrographs of PAN-based ACF samples both at the surface and cross-sections are shown in Fig. 4. For sample A2, elongated micropores were observed parallel to the fiber axis, similar to Daley's results [12]. The micropore size (from the adsorption measurement) is about several ångströms. This oriented microporous structure may result from the shear associated with melt spinning of the original fiber precursor. For sample A4, a highly mesoporous structure with a small fraction of macropores was observed and mesopores were randomly distributed with respect to the fiber axis. The electron micrographs indicated that the porous structure is relatively stable and homogen-

eous. The initial pores which were formed during carbonization begin to widen when exposed to steam/carbon dioxide due to diffusion of these etchants into the fiber bulk. These small micropores are created by the evolution of volatile species. The stability of these species is directly related to the stability and persistence of the cross-linked structure in the precursor fiber [13].

3.3 Dubinin-Radushkevich equation results

It is now generally agreed that physisorption within the narrowest micropores does not involve monolayer formation, but instead takes place preferentially at very low P/P_0 (initially around $P/P_0 \sim 10^{-5}$). This process is associated with enhanced adsorbent-adsorbate interactions and results in an appreciable distortion of the adsorption isotherm [14]. Adsorption in microporous carbon occurs by primary micropore filling; Dubinin and his group originally modeled microporous adsorption using the Polanyi potential theory. Dubinin and Radushkevich proposed an equation under assumption of volume filling which is written as follow:

$$V = V_0 \exp \left[-(A/E)^2 \right]$$

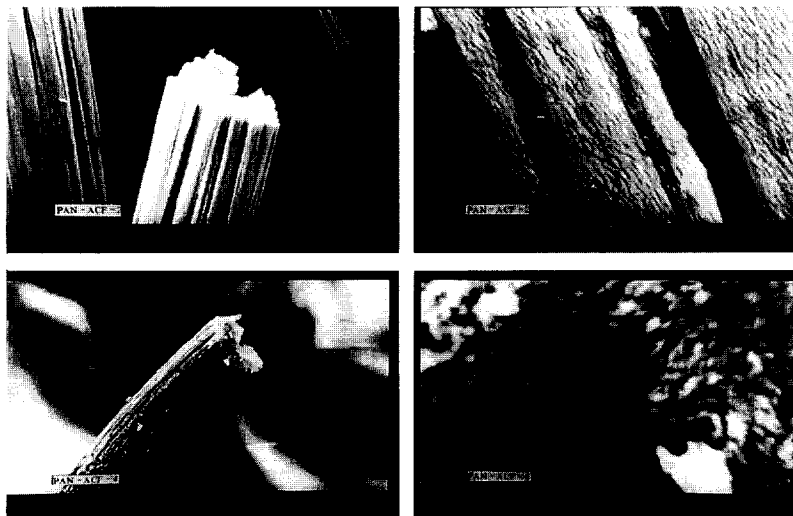


Fig. 4. Scanning electron micrographs of PAN-based ACFs

where V is the amount adsorbed at relative pressure P/P_0 , V_0 is the micropore volume; $A = RT \ln(P/P_0)$ is the adsorption potential, where R is the gas constant, T is absolute temperature; E is an energy constant which can be factorized in a characteristic adsorption energy, E_0 , which relates to the adsorbent; and an affinity coefficient, β , which is a constant for a given adsorptive, $E = \beta E_0$ [15,16].

The characteristic energy E_0 appears to be an inverse function of the average pore size, as suggested by the adsorption of molecules of different sizes from the vapor and the liquid phase. On the basis of preliminary data, Dubinin and Stoeckli [4] suggested the relation, $E_0 = K/x$, between the characteristic adsorption energy and the average half-width x of the slit-shaped pores, on average, K equals 12.0 kJ mol^{-1} [17].

The characteristic adsorption energy E for nitrogen at 77.4 K is determined according to Dubinin–Radushkevich transformed isotherm plots in which two linear sections are apparent, as shown in Fig. 5. At this point, two characteristic adsorption energies are obtained. Taking the affinity coefficient of nitrogen as 0.33, (benzene as the standard vapor, $\beta = 1$) the pore half-width x of slit-shaped micropores is calculated using the Dubinin method, as listed in Table 2. Kaneko and his co-workers [18,19] have noted that some Dubinin–Radushkevich plots exhibit a succession of linear regions. These features are interpreted in terms of a multi-stage mechanism of micropore filling, i.e. an extension of the principles of primary and cooperative micropore filling. The Dubinin–Radushkevich plots are assumed to be caused by the different micropore structures. Marsh [20] and Rand [21] suggested that the negative deviations at low relative pressure were due to acti-

vated diffusion effects, because the adsorbate molecules are excluded from the smallest sizes of the microporosity by kinetic effects. The kinetic energy of adsorbate molecules is insufficient to penetrate fully the micropore space at low adsorption temperature, e.g. 77 K; the rate of adsorption becomes so slow as to be undetectable over periods of hours and days [20,22]. We propose that there is no reason why the excluded adsorbate molecules at low relative pressure and low adsorption temperature don't enter the larger micropores, such as supermicropores, at the surface of ACFs. With the relative pressure and/or adsorption temperature increasing the adsorbate molecules subsequently diffuse into the ultramicropores in the bulk of ACFs. The differences between micropores at the surface and in the bulk of ACFs are observed by scanning tunneling microscopy (STM), as described by Daley *et al.* [13]. The average pore half-widths derived from the characteristic adsorption energies of nitrogen isotherms are in agreement with the values from the Horvath–Kawazoe equation and the DFT method.

4. CONCLUSIONS

PAN-based ACFs exhibit bimodel or trimodel micropore distributions which are divided into two sections of $>1 \text{ nm}$ (supermicropore) and $<0.7 \text{ nm}$ (ultramicropore). The pore size increases and pore size distributions become broader with increasing specific surface area. The DFT method allows pore size distribution to be determined over a wide range from micropore to macropore using a single analysis method. The analysis results by means of different methods are in good agreement with one another.

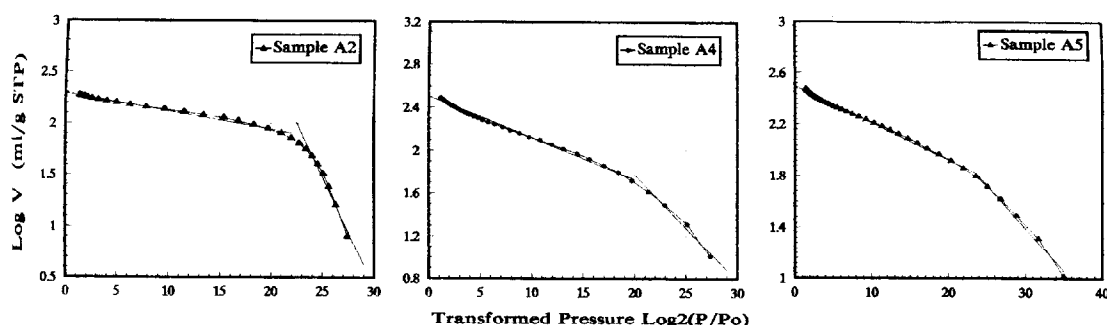


Fig. 5. Dubinin–Radushkevich plots for the nitrogen adsorption at 77.4 K by PAN-based ACFs

Table 2. Characteristics of porous structure of PAN-based ACFs by Dubinin–Radushkevich plots

Sample	E_1 (kJ mol^{-1})	X_1 (nm)	r_1	E_2 (kJ mol^{-1})	X_2 (nm)	r^2
A2	7.40	0.535	0.996	2.37	1.687	0.991
A4	5.20	0.762	0.991	2.63	1.505	0.988
A5	6.05	0.651	0.998	3.61	1.096	0.995

r^2 is the linear correlation coefficient.

REFERENCES

1. Suzuki, M., *Carbon*, 1994, **32**(4), 577.
2. Ishizaki, N., *Chem. Eng.*, 1984, **29**(7), 496.
3. Brunauer, S., Emmett, P. and Teller, E., *J. Am. Chem. Soc.*, 1938, **60**, 309.
4. Dubinin, M. M. and Stoeckli, H. F., *J. Colloid Interface Sci.*, 1980, **75**, 34.
5. Horvath, G. and Kawazoe, K., *J. Chem. Eng. Jpn.*, 1983, **16**(8), 470.
6. Seaton, N. A., Walton, J. P. R. B. and Quirk, N., *Carbon*, 1989, **27**(6), 853.
7. Oliver, J. P., Conklin, W. B. and Szombathely, M. v., *Characterization of Porous Solids III*, ed. J. Rouquerol, F. Rodriguez-Reinoso, K. S. W. Sing and K. K. Unger. Elsevier, Amsterdam, 1994, p. 81.
8. Kruk, M., Jaroniec, M. and Berezniński, Y., *J. Colloid Interface Sci.*, 1996, **182**, 282.
9. Maozhang Wang, Jingtang Zheng, Pingguang Liu, Fu He and Zhenyu Ryu, Chinese Patent ZI 94 2 45396.4, 1994.
10. Gregg, S. J. and Sing, K. S. W., *Adsorption, Surface Area and Porosity*, 2nd edn. Academic Press, London, 1982.
11. Latoskie, C., Gubbins, K. E. and Quirk, N., *Characterization of Porous Solids III*, ed. J. Rouquerol, F. Rodriguez-Reinoso, K. S. W. Sing and K. K. Unger. Elsevier, Amsterdam, 1994, p. 51.
12. Daley, M. A., Tandon, D., Economy, J. and Hippo, E. J., *Carbon*, 1996, **34**(10), 1191.
13. Daley, M. A., Tandon, D., Economy, J. and Hippo, E. J., *Preprint of ACS, Division of Fuel Chemistry*, 1996, **41**(1), 326.
14. Sing, K. S. W., *Characterization of Porous Solids II*, ed. F. Rodriguez-Reinoso, J. Rouquerol, K. S. W. Sing and K. K. Unger. Elsevier, Amsterdam, 1991, p. 1.
15. Stoeckli, H. F., Kraehenbuehl, F., Ballerini, L. and De Bernardini, S., *Carbon*, 1989, **27**(1), 125.
16. Bradley, R. H. and Rand, B., *J. Colloid Interface Sci.*, 1995, **169**, 168.
17. Dubinin, M. M., *Carbon*, 1987, **25**(5), 593.
18. Kakei, K., Ozeki, S., Suzuki, T. and Kaneko, K., *J. Chem. Soc. Faraday Trans.*, 1990, **86**(2), 371.
19. Kakei, K., Ozeki, S., Suzuki, T. and Kaneko, K., *Characterization of Porous Solids II*, ed. J. Rouquerol, F. Rodriguez-Reinoso, K. S. W. Sing and K. K. Unger. Elsevier, Amsterdam, 1991, p. 429.
20. Marsh, H., *Carbon*, 1987, **25**(1), 49.
21. Rand, B., *J. Colloid Interface Sci.*, 1976, **56**(2), 337.
22. McEnaney, B. and Mays, T. J., *Introduction of Carbon Science*. Butterworths, London, 1989, p. 173.